Title
Envelope Code for Electrostatically Accelerated Beam with ESQ Focusing

Authors
Soroka, L.
Anderson, O.A.

Publication Date
1993-02-01

LBL-33678
UC-420

Lawrence Berkeley Laboratory
UNIVERSITY OF CALIFORNIA

Accelerator & Fusion
Research Division

Presented at the Computational Accelerator Physics Conference,
Pleasanton, CA, February 22–26, 1993, and to
be published in the Proceedings

Envelope Code for Electrostatically Accelerated Beam with ESQ Focusing

L. Soroka and O.A. Anderson

February 1993

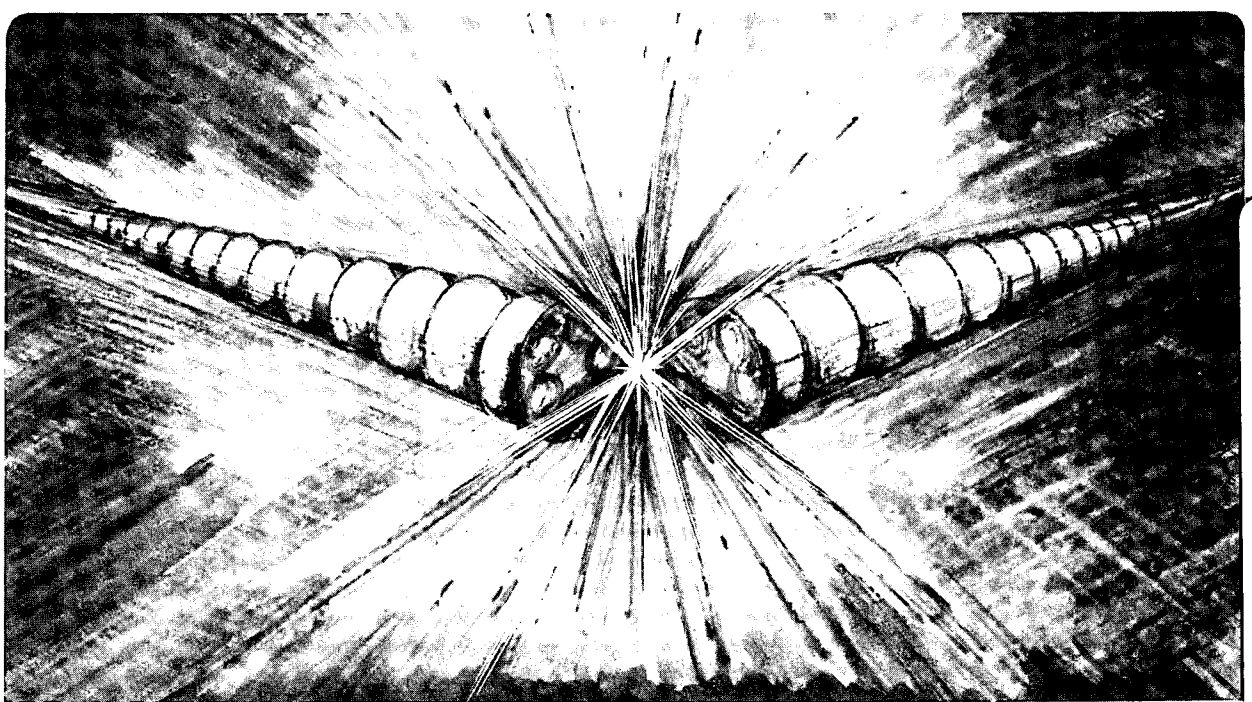

Prepared for the U.S. Department of Energy under Contract Number DE-AC03-76SF00098

DISCLAIMER

LBL-33678
UC-420

ENVELOPE CODE FOR ELECTROSTATICALLY ACCELERATED BEAM WITH ESQ FOCUSING

L. Soroka and O. A. Anderson

Lawrence Berkeley Laboratory
University of California
Berkeley, CA 94720

February 1993

Presented at the Computational Accelerator Physics Conference
Hilton at the Club
Pleasanton, CA
February 22-26, 1993

This work was supported by the Director, Office of Energy Research, Office of Fusion Energy, Development and Technology Division, of the U.S. Department of Energy under Contract No. DE-AC03-76SF00098.

ENVELOPE CODE FOR ELECTROSTATICALLY ACCELERATED BEAM WITH ESQ FOCUSING

L. Soroka and O. A. Anderson
Lawrence Berkeley Laboratory, Berkeley CA 94720

ABSTRACT

We present a new envelope code, "ESQACL," which we have used for designing ESQ-focused ion or electron accelerators and transport systems. This code uses improved envelope equations and also allows the option of using accurate field maps along the beam axis instead of typical models. We show how the transverse fields are handled in the different cases. ESQACL is designed to interact with a 3-D Laplace solver that provides the fields of the complete system of electrodes including their supporting structure. We show examples that contrast results from this new code with those obtained from traditional envelope equations, from traditional field models, and from a particle code.

INTRODUCTION

The code described here has been used to design a number of accelerators and transport systems, including: a 200 kV CCVV prototype accelerator [1] built and tested by the MFE group at LBL; a 1 MV accelerator for a proposed test facility [2]; a 1.3 MV, 1A D^- accelerator channel for ITER [3]; a high-current electron accelerator for an FEL [4]; and an injector proposed for SSC and CERN [5]. ESQACL would also be suitable for designing ESQ-focused heavy ion accelerators.

In the next section we discuss the special features of our code, including our improved envelope equations [6] and the available field options. The options are: (a) accurate fields from a 3-D Laplace solver, which ESQACL combines in proportion to user-specified electrode voltages; (b) an arbitrary field model supplied by user; or (c) fields from ESQACL's own associated trapezoidal field module.

We then discuss the treatment of transverse fields for the different field models, the code structure, and examples of applications. The examples contrast results from this new code with those obtained from traditional envelope equations [7,8], from traditional field models [9], and from a particle code [10].

FIELD MODELS AND ENVELOPE EQUATIONS

ESQACL accepts two types of external field maps; alternatively, it can stand alone and generate its own a trapezoidal map. When a certain flag [11] is set to 0, the code takes a set of input field maps (on axis) from a 3-D Laplace solver. For each Laplace calculation used in the set of maps, a single quadrupole pair with support plate was activated with unit voltage while all the other electrodes were grounded. There are as many Laplace field maps as there are independent voltages in the channel. These separate fields are combined by ESQACL in proportion to electrode voltages specified as input.

When the field map flag = 1, the user supplies the fields on axis for the entire system; these could by obtained, for example, from a single Laplace run for fixed electrode voltages. When the flag = 2, ESQACL calculates the fields internally using the trapezoidal field model [9]. The first and third options allow interactive optimization of the electrode voltages.

The Laplace fields and trapezoidal fields are compared in Fig. 1 for the CCVV prototype accelerator [1], [2] in which the ESQ electrodes are supported by end plates. In the trapezoidal case, the potential along the axis (dotted line in Fig. 1a) is set at the mean electrode potential in the overlapping quadrupole region and ramps linearly to the plate potential in the nonoverlapping part. It ramps linearly again between the support plates for the different cells, which are at different potentials for beam acceleration. The actual Laplace field (the solid line) is, of course, much smoother. Transverse field gradients are shown in Figs. 1b and 1c. The trapezoidal model (1c) shows linear ramps in the nonoverlapping regions and constant values in the overlapping regions. On the other hand, the realistic Laplace maps (1b) show a large shielding effect from the support plates. In a later section we show that the beam envelopes for the fields in Figs. 1b and 1c are not greatly different, providing that our improved envelope equations are used. Presumably, this similarity in the envelopes is due to the fact that if the Laplace gradients G_x and G_y are suitably averaged, they do resemble the trapezoidal models.

The improved envelope equations used by ESQACL were derived in Ref. [6] and are reproduced here in the appendix. These equations describe a relativistic uniformly charged warm beam which experiences a combination of axisymmetric and quadrupole focusing forces as well as *longitudinal acceleration.* The forces are assumed to be electrostatic, although the code could easily be generalized to include magnetic focusing. The derived equations are more general than those previously published. In particular, a focusing term proportional to the second derivative of the potential along the beam axis is included for improved accuracy when field models are used. (This term has been previously omitted in equations involving both ESQ focusing and space charge [7,8,9].) Since the potential on axis is a basic quantity in an electrostatic accelerator, the envelope equations, including relativistic factors, are written directly in terms of the potential (see appendix).

To facilitate comparisons of ESQACL results with those obtained from other envelope equations, field models, and codes [7,8,9,10], we include two switches. One turns on/off the relativistic effects, and the other turns on/off the axial electric field gradient effect. Reference [11] describes other input features of our code.

TRANSVERSE FIELDS: REAL FIELD MAP vs SIMPLIFIED FIELD MODEL

The Laplace and trapezoidal alternatives accepted by ESQACL (discussed above and illustrated in Fig. 1) require two different approaches for calculating the transverse focusing in the paraxial approximation:

(a) Field map: In this mode, the potential and the required gradients along the axis are obtained from an external Laplace solver (or, in principle, from measurements on actual hardware). Near the axis, the transverse fields increase linearly:

$$E_x^{vac} = -G_x(0,0,z)x$$
$$E_y^{vac} = -G_y(0,0,z)y.$$

The Laplace solver calculates G_x and G_y and passes them to ESQACL.

(b) Simplified models: In this mode, the vacuum potential is divided into a part with axisymmetry and a part with quadrupole symmetry; Taylor expansion gives [6]

$$V^{vac}(x,y,z) = V(0,0,z) + G_A(z)\,\frac{x^2+y^2}{2} + G_Q(z)\,\frac{x^2-y^2}{2} + \cdots .$$

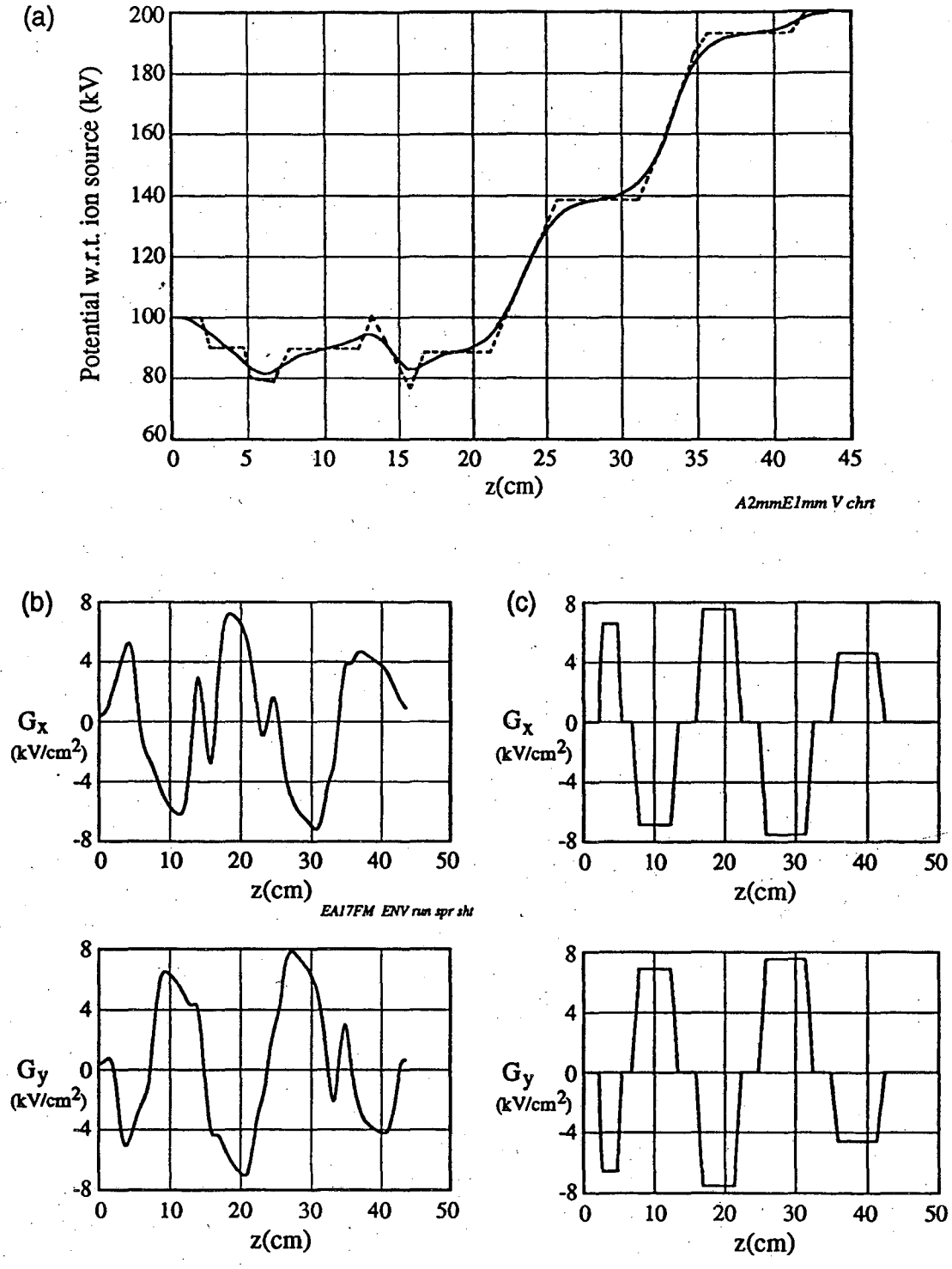

Fig. 1. (a) Potential on axis for CCVV accelerator prototype: actual (solid line); trapezoidal model (dashed). Either is available with ESQACL. (b) Transverse field gradients for actual ESQ-focused accelerator. (c) Transverse field gradients provided by ESQACL's trapezoidal model.

The axisymmetric coefficient G_A arises from the acceleration fields through Laplace's equation. We have [6] $G_A(z) = (1/2)E_z'$, where E_z' stands for $-V''(0,0,z)$, so that

$$E_x^{vac} = -\frac{1}{2}E_z'x - G_Q(z)x,$$

$$E_y^{vac} = -\frac{1}{2}E_z'y + G_Q(z)y,$$

where the quadrupole gradient is

$$G_Q(z) = \frac{2V_Q}{a_Q^2}$$

in terms of the quadrupole radius a_Q and the quadrupole voltage V_Q. Note that the E_z' term is missing in most treatments that include G_Q, but appears in our envelope equations (see appendix) where the notation $-V''$ is used for E_z'. (This V'' term is not used in the field map mode, because it is already included in the G_x and G_y maps).

THE CODE

ESQACL runs on any Macintosh computer with enough memory to accomodate MacFortran. The code has six principal modules: input; V_Q setup; main module; trapezoidal map generator; output; and graphics.

The basic input file contains lattice information (quadrupole lengths, overlaps, and gaps; support-aperture sizes and gaps); initial integration step; x- and y-plane voltages; beam current and rms emittance; initial radii and entrance angles in the x- and y-planes; mass and charge for the beam particles. If the field map flag = 0 or 1, external maps must be supplied. If the flag = 2, a trapezoidal field map is generated using information from the basic input file. In all cases the lattice geometry input is used for the graphical display of the results of the simulations.

The V_Q setup module computes focusing voltages V_Q from the input voltages specified for each electrode. These are used for the trapezoidal field map and as coefficients for superposition of the multiple maps when the field map flag = 0.

The main module is modular itself. It starts with a pre-cycle stage. Regardless of the model chosen, the result of the pre-cycle stage is always a field map input for the next stage—the cycle. The cycle contains a main z-stepping loop for Runga-Kutta-Gill integration, a type suitable for the variable mesh size typically encountered. The last main stage requests outputs and plots of the results. Interactive dialog for altering the V_Q's can be used for rapid design optimization. Special modules exist to dump the field map and update the input if it is changed during the interactive design run.

EXAMPLES

Figure 2a shows particle trajectories for the 200 keV CCVV prototype accelerator [1] using the 3-D self-consistent particle code Argus [10]. Argus was then run without beams (a much quicker process) to generate a set of axial vacuum-field maps, one for each pair of electrodes, as described earlier. ESQACL combined these maps in proportion to the electrode voltages used for Fig. 1a, thus producing the envelopes of Fig. 1b. These are nearly identical to the envelopes of the particle trajectories (except that the y trajectories at the exit in Fig 2a are badly aberrated, an effect not treated by the envelope equations). The comparison between

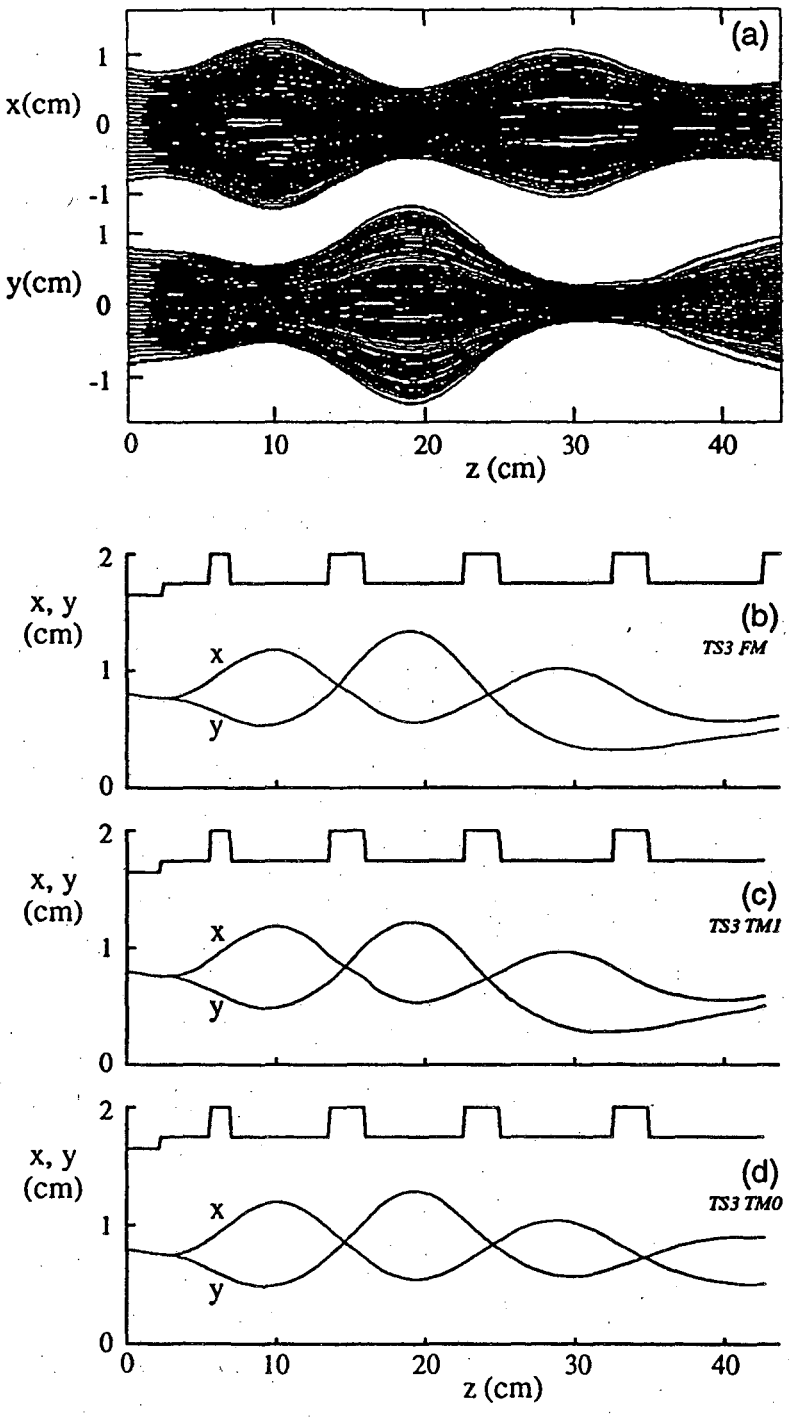

Fig. 2. (a) Particle trajectories in prototype 200 keV CCVV accelerator using Argus code; (b) ESQACL calculation for same electrode voltages using Laplace field maps; (c) same but using the trapezoidal field model; (d) same with V″ term omitted.

ARGUS and ESQACL is especially stringent because in this example the beam is mismatched. Since the particle calculation takes several hours of Cray time, one sees the tremendous advantage of having an accurate envelope code (which runs almost instantaneously on a Macintosh IIci) for optimization runs.

Similar envelopes are obtained (Fig. 2c) from the trapezoidal model when the V″ (gap focus) term of ESQACL is included. When that term is dropped (Fig. 2d), the envelopes are quite inaccurate.

ESQACL's trapezoidal map option was used to model a 100 keV LEBT (low-energy beam transport system) [5]. This system was designed to deliver a round beam at the exit. We compare results from ESQACL (Fig. 3a) with results from a previous code [9] where the V″ term was omitted (Fig. 3b). The neglect of additional focusing from the V″ term is detrimental, even for this transport system, because the electrode support plates and non-overlapping regions produce gap-focus effects.

A 100-A megavolt electron accelerator [4] based on a 1-A D^- accelerator channel [3] is modeled in Fig. 4a. The relativistic corrections involving ν (see appendix) are dominant for this case, as seen by comparison with Fig. 4b where these factors are set equal to unity. Figure 4a shows how easily ESQ' s focus electrons —the current is 100 times larger than with D^-. The V_Q's actually *decrease* at higher beam energies, in a way that can be described analytically [4].

ACKNOWLEDGMENTS

We are grateful to Charles Kim for providing his original envelope code and showing us how to use it. (He was co-author on several of our papers in 1987 and 1988.) Although we have completely restructured the code and introduced new features such as external field maps, fully relativistic factors, and the gap focusing effect, we have retained most of Dr. Kim's nomenclature. We would also like to thank Ken Klubok for his assistance in making the code more user friendly, finding bugs, and doing the runs for Fig. 4.

This work was supported by the Director, Office of Energy Research, Office of Fusion Energy, Development and Technology Division, of the U.S. Department of Energy under Contract No. DE-AC03-76SF00098.

REFERENCES

[1] O.A. Anderson, W.S. Cooper, W.B. Kunkel, J.W. Kwan, R.P. Wells, C.A. Matuk, P. Purgalis, L. Soroka, M.C. Vella, G.J. De Vries, and L.L. Reginato, "The CCVV High-Current Megavolt Range DC Accelerator," Proceedings of 1989 Particle Accelerator Conf., Chicago, March 20-23, 1989; IEEE Cat. No. 89CH2669-0, p. 1117.

[2] O.A. Anderson, L. Soroka, et al., "Applications of the Constant-Current Variable-Voltage DC Accelerator," Nucl. Instrum. and Meth. B40/41, 877 (1989).

[3] O.A. Anderson, et al., "Negative Ion Source and Accelerator Systems for Neutral Beam Injection in Large Tokamaks," in *Plasma Physics and Controlled Nuclear Fusion Research 1990*, Proc. 13th IAEA Plasma Physics and Controlled Fusion Conf.,Washington DC, International Atomic Energy Agency, Vienna, 1991, p. 503.

[4] O.A. Anderson, L. Soroka, P.W. Van Amersfoort, W.H. Urbanus, "A High-Current MV DC Electron Accelerator," oral presentation at the 1991 IEEE Particle Accelerator Conference, May 6-9, 1991, San Francisco; LBL-29897a.

[5] O.A. Anderson, L. Soroka, J.W. Kwan, and R.P. Wells, "Application of Electrostatic LEBT to High Energy Accelerators," Proc. 2nd European Particle Accelerator

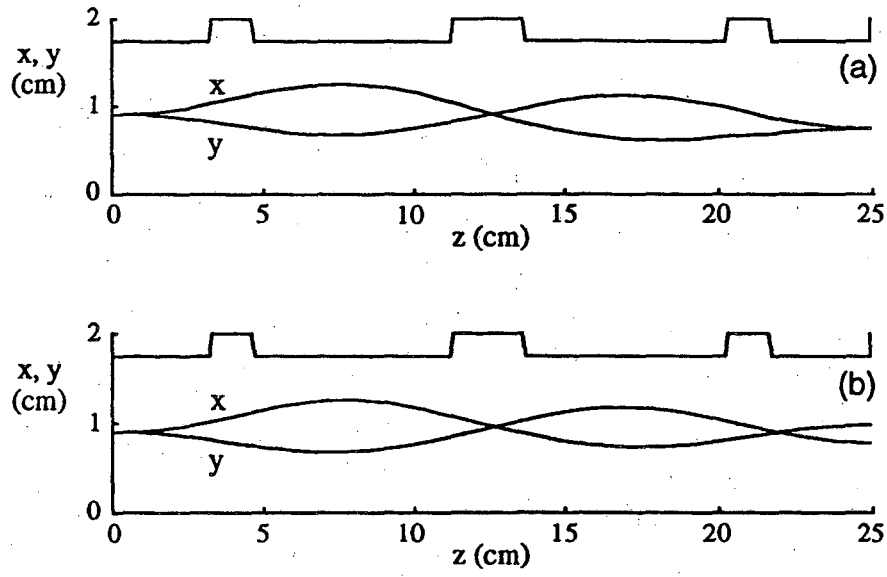

Fig. 3. (a) ESQACL calculation for 100-keV 4-quad LEBT using trapezoidal field model.
(b) Calculation for same case but with V″ term omitted (cf. Appendix A).

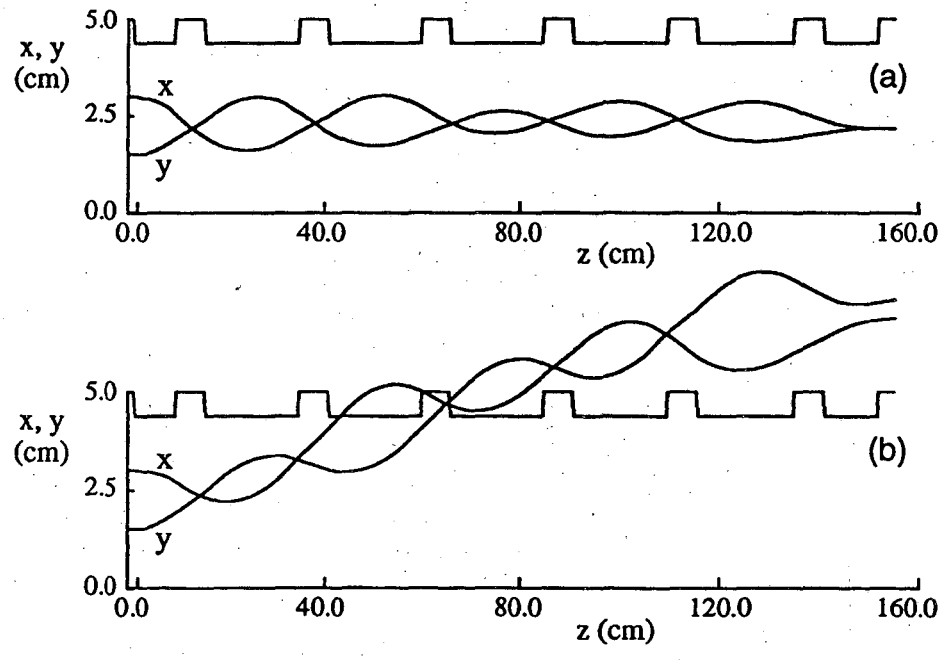

Fig. 4. (a) ESQACL calculation for 1-MeV 100-A electron accelerator.
(b) Calculation for same case but with relativistic factors set equal to unity; see text.

Conference, Nice, France, June 12 - 16, 1990; P. Marin and P. Mandrillon, Editors; Editions Frontières, Gif-sur-Yvette, 1990, p. 1288.

[6] O.A. Anderson, "Envelope Equations for Electrostatically Accelerated Beam with ESQ Focusing," Lawrence Berkeley Laboratory report LBL 30304.

[7] J.D. Lawson, "Space Charge Optics," in *Applied Charged Particle Optics*, A. Septier, Ed., Academic Press, New York, 1983.

[8] J.D. Lawson, *The Physics of Charged-Particle Beams,* Second Edition, Oxford University Press, 1988.

[9] C.H. Kim, Envelope code with acceleration, personal communication, Lawrence Berkeley Laboratory, 1987.

[10] A. Mankofsky, "Three-Dimensional Electromagnetic Particle Codes and Applications to Accelerators," Linear Accelerator and Beam Optics Codes, C.R. Eminheizer, Ed., A.I.P. Conf. Proc. No. 177, 1988, p. 137.

[11] L. Soroka and O.A. Anderson, "Users Manual for ESQACL Code," Lawrence Berkeley Laboratory report PUB-3096.

APPENDIX

The envelope equations used by ESQACL are derived in Ref. [6], where the necessary assumptions are discussed. We use the symbols: proton charge = e, particle charge = q = Ze, proton mass = m_p, particle rest mass = $m_0 = Am_p$, speed of light = c, electrostatic potential *normalized to zero at source* = V, and

$\upsilon = -\dfrac{qV}{m_0c^2} > 0$ — Fractional increase in particle mass; normalized potential

$\epsilon_N \equiv \beta\gamma\epsilon$ — Normalized emittance of beam.

Our envelope equations are

$$a' = a_p \tag{1a}$$

$$a_p' = -\frac{1+\upsilon}{1+\frac{\upsilon}{2}}\left(\frac{V'a_p}{2V}+\frac{V''a}{4V}-\frac{V_Q a}{Va_Q^{\,2}}\right)-\frac{1}{\left(1+\frac{\upsilon}{2}\right)^{\frac{3}{2}}}\frac{1}{\upsilon^{\frac{1}{2}}V}\frac{2^{-\frac{3}{2}}}{\pi\varepsilon_0 c}\frac{I}{a+b}+\frac{1}{1+\frac{\upsilon}{2}}\frac{\epsilon_N^{\,2}}{2\upsilon a^3} \tag{1b}$$

$$b' = b_p \tag{1c}$$

$$b_p' = -\frac{1+\upsilon}{1+\frac{\upsilon}{2}}\left(\frac{V'b_p}{2V}+\frac{V''b}{4V}+\frac{V_Q b}{Va_Q^{\,2}}\right)-\frac{1}{\left(1+\frac{\upsilon}{2}\right)^{\frac{3}{2}}}\frac{1}{\upsilon^{\frac{1}{2}}V}\frac{2^{-\frac{3}{2}}}{\pi\varepsilon_0 c}\frac{I}{a+b}+\frac{1}{1+\frac{\upsilon}{2}}\frac{\epsilon_N^{\,2}}{2\upsilon b^3}. \tag{1d}$$

Each of the three terms on the right of (1b) or (1d) is preceeded by a relativistic correction factor (involving $1+\upsilon/2$ and in one case $1+\upsilon$), which approaches unity in the nonrelativistic case. Our code includes an input switch [11], which can set all these terms equal to unity and allow comparisons with nonrelativistic codes.

LAWRENCE BERKELEY LABORATORY
UNIVERSITY OF CALIFORNIA
TECHNICAL INFORMATION DEPARTMENT
BERKELEY, CALIFORNIA 94720